JOURNAL OF VIROLOGY, July 2006, p. 6936–6942 Vol. 80, No. 14
0022-538X/06/$08.00+0 doi:10.1128/JVI.00243-06
Copyright © 2006, American Society for Microbiology. All Rights Reserved.

The Double-Stranded RNA Binding Protein 76:NF45 Heterodimer Inhibits Translation Initiation at the Rhinovirus Type 2 Internal Ribosome Entry Site

Melinda K. Merrill and Matthias Gromeier*

Department of Molecular Genetics and Microbiology, Duke University Medical Center, Durham, North Carolina 27710

Received 2 February 2006/Accepted 4 April 2006

Poliovirus (PV) plus-strand RNA genomes initiate translation in a cap-independent manner via an internal ribosome entry site (IRES) in their 5′ untranslated region. Viral translation is codetermined by cellular IRES *trans*-acting factors, which can influence viral propagation in a cell-type-specific manner. Engineering of a poliovirus recombinant devoid of neuropathogenic properties but highly lytic in malignant glioma cells was accomplished by exchange of the cognate poliovirus IRES with its counterpart from human rhinovirus type 2 (HRV2), generating PV-RIPO. Neuroblast:glioma heterokaryon analyses revealed that loss of neurovirulence is due to *trans*-dominant repression of PV-RIPO propagation in neuronal cells. The double-stranded RNA binding protein 76 (DRBP76) was previously identified to bind to the HRV2 IRES in neuronal cells and to inhibit PV-RIPO translation and propagation (M. Merrill, E. Dobrikova, and M. Gromeier, J. Virol. 80:3347–3356, 2006). The results of size exclusion chromatography indicate that DRBP76 heterodimerizes with nuclear factor of activated T cells, 45 kDa (NF45), in neuronal but not in glioma cells. The DRBP76:NF45 heterodimer binds to the HRV2 IRES in neuronal but not in glioma cells. Ribosomal profile analyses show that the heterodimer preferentially associates with the translation apparatus in neuronal cells and arrests translation at the HRV2 IRES, preventing PV-RIPO RNA assembly into polysomes. Results of this study suggest that the DRBP76:NF45 heterodimer selectively blocks HRV2 IRES-driven translation initiation in neuron-derived cells.

Eukaryotic mRNA translation regulation is most often achieved by interference with initiation events (10). Unimpeded initiation occurs upon assembly of eukaryotic initiation factor 4F at the cap, recruitment of the 43S preinitiation complex, scanning, formation of the 48S initiation complex at the initiation codon, and 60S ribosomal subunit joining. Translation initiation repressors binding to 5′ and 3′ untranslated regions (UTR) have been reported to interfere with distinct steps of the initiation cascade. These include obstructed eukaryotic initiation factor 4F cap assembly (26), inhibited stable association of the 40S ribosomal subunit (9, 12), and blocked 60S ribosomal subunit joining (31).

Some mRNAs, however, can initiate translation by noncanonical mechanisms. Picornaviruses feature uncapped (29) plus-strand RNA genomes whose translation depends on internal ribosome entry sites (IRES) within their highly structured 5′ UTR for initiation in a 5′-end, cap-independent manner (21, 34). Poliovirus (PV), a member of the family *Picornaviridae*, is responsible for paralytic poliomyelitis, resulting from specific targeting of spinal cord motor neurons in the human central nervous system. Neurological disease is the result of complex interactions determined by the host, e.g., aggravating susceptibility factors (44), viral receptors in the central nervous system (17), and the innate immune response (19), and the virus itself, e.g., capsid structure (43) and the viral RNA-dependent RNA polymerase (33; reviewed in reference 16).

* Corresponding author. Mailing address: Dept. of Molecular Genetics & Microbiology, Duke University Medical Center, Box 3020, Durham, NC 27710. Phone: (919) 668-6205. Fax: (919) 684-8735. E-mail: grome001@mc.duke.edu.

An important viral determinant of neuropathogenesis is the IRES. Single point mutations in IRES stem loop domain V of the PV (Sabin) oral vaccine strains have been implicated in neurovirulence attenuation (8, 22, 37), and deliberate manipulation of the PV IRES reduces its neurovirulent potential (1). Replacement with a heterologous IRES element of human rhinovirus type 2 (HRV2) eliminates PV propagation in cells of neuronal derivation (5, 13, 14) and abolishes neuropathogenicity in mice transgenic for the human PV receptor (13) and in nonhuman primates (14). Despite severely repressed viral propagation in neurons, the chimeric PV-RIPO replicates with wild-type kinetics in malignant glioma (15) and breast cancer (30) cells. These observations suggest that the conditions for HRV2 IRES-mediated translation in neurons differ from those in glioma and other cancer cells. HRV2 IRES-driven translation could require enabling factors in glioma cells that are absent in neuronal cells, or, alternatively, negative regulators in neurons could block PV-RIPO propagation.

Neuroblast:glioma heterokaryon analyses revealed that neuron-specific repression is *trans* dominant over robust PV-RIPO propagation in glioma cells (27). We identified association of double-stranded RNA binding protein 76 (DRBP76), nuclear factor of activated T cells, 45 kDa (NF45), and RNA helicase A (RHA) with the HRV2 IRES by affinity chromatography with lysates from neuron-derived cells (27). These proteins have been reported to associate with each other in diverse molecular arrangements: the DRBP76 monomer, a DRBP76:NF45 heterodimer, and a DRBP76:NF45:RHA heterotrimer also known as the nuclear factor associated with double-stranded RNA (NFAR) complex. Only DRBP76 and RHA are RNA binding proteins, suggesting that association of NF45 with the HRV2 IRES is indirect. DRBP76 and NF45 are sub-

stantially more abundant in cytoplasmic fractions of neuronal cells than in those of glioma cells and are enriched in the ribosomal salt wash (RSW). Therefore, we investigated DRBP76 as a putative HRV2 IRES *trans*-acting factor. RNA interference-mediated depletion of DRBP76 in neuronal cells revealed its role in cell-type-specific restriction of PV-RIPO growth (27).

Here we report that DRBP76 exists in a heterodimeric complex with NF45 in neuronal but not in glioma cells and that this complex specifically interacts with the HRV2 IRES in the former. Importantly, the heterodimer preferentially associates with the translation apparatus in neuronal but not in glioma cells. We demonstrate that PV-RIPO genomic RNA is translationally arrested in neuronal cells, whereas efficient assembly into polysomes occurs in glioma cells. Our observations suggest that interaction of the HRV2 IRES with the DRBP76:NF45 complex in neuronal cells contributes to translation arrest at the IRES, thus preventing viral translation and propagation in a cell-type-specific manner.

MATERIALS AND METHODS

cDNA, in vitro transcription, cell culture, and virus infections. Vectors for in vitro transcription of HRV2 IRES RNAs and for pshDRBP76, encoding a retroviral vector expressing short hairpin RNA (shRNA) complementary to DRBP76 mRNA, were generated as described previously (27). Cell culture and propagation, virus infections, and growth assays were performed essentially as described before (13–15).

Cell extract preparation and Western blotting. S10 lysates of HEK-293 and HTB-14 cells were prepared as described before (27). Lysates (6 ml at 0.5 mg/ml) were purified over 3-ml heparin Sepharose columns (CL4B heparin Sepharose; Roche, Indianapolis, IN) before use with RNA affinity chromatography to reduce the level of nonspecific nucleic acid binding proteins. Western blotting was performed as described before (6), with primary antibodies including mouse anti-DRBP76 (α-DRBP76) (Transduction Laboratories, San Jose, CA), rabbit α-RHA (a gift from J. Hurwitz, Memorial Sloan Kettering Cancer Center), rabbit α-NF45 (a gift from S. Behrens, Fox Chase Cancer Center), murine α-tubulin (Sigma, St. Louis, MO), and rabbit α-ribosomal protein S6 (α-RpS6) (Cell Signaling, Beverly, MA).

Molecular size exclusion chromatography. A 24-ml Superdex 200 HR 10/30 column (Amersham Biosciences, Piscataway, NJ) was equilibrated in running buffer (50 mM Tris-HCl, pH 7.5, 100 mM KCl) and calibrated with molecular size standards blue dextran (2 MDa), apoferritin (443 kDa), β-amylase (200 kDa), alcohol dehydrogenase (150 kDa), albumin (66 kDa), and carbonic anhydrase (29 kDa) according to the manufacturer's protocol (Sigma, St. Louis, MO). Protein was applied to the column under constant pressure at 0.5 ml/min by using a fast-performance liquid chromatography system. One-milliliter fractions were collected, and the protein concentration was determined by Bradford analysis (2a). S10 lysate was diluted to 5 mg/ml in running buffer with 5% glycerol to a final volume of 100 μl. Protein was trichloroacetic acid precipitated from every fraction and analyzed by sodium dodecyl sulfate-polyacrylamide gel electrophoresis (SDS-PAGE) followed by Western blotting.

Immunoprecipitation and immunodepletion. Immunoprecipitation was performed as described previously (27). Briefly, 35-mm dishes of confluent cells were lysed in 200 μl radioimmunoprecipitation assay buffer (27) and subjected to immunoprecipitation with α-DRBP76 at 5 μg/ml, α-NF45 at 1:100, or mouse immunoglobulin G at 5 μg/ml. After extensive washing, protein was recovered with 1% SDS and analyzed by SDS-PAGE followed by Western blotting. Immunodepletion was performed as described previously (41), with the following modifications. One milliliter of 50% protein G beads (Amersham Pharmacia, Piscataway, NJ) in PB {20 mM HEPES, pH 7.4, 120 mM potassium acetate (KOAc), 4 mM magnesium acetate [$Mg(OAc)_2$], 5 mM dithiothreitol (DTT)} was coupled to 3 mg α-DRBP76 antibody overnight at 4°C. One hundred microliters of antibody-conjugated beads was incubated with 2 mg HEK-293 S10 extract for 30 min on ice with occasional mixing. The protein G beads were removed by centrifugation. This procedure was repeated four times to remove the protein.

Density gradient centrifugation and ribosomal profiles. Cell lysates were prepared as described before (24). Cells were mock infected or infected with PV-RIPO at a multiplicity of infection of 10. At 4 hours postinfection (hpi), cycloheximide (CHX) (Sigma, St. Louis, MO) was added to the growth media (0.2 mM for 15 min) at 37°C. The cells were collected in 15 ml of permeabilization buffer [110 mM KOAc, 25 mM HEPES, 2.5 mM $Mg(OAc)_2$, 1 mM EGTA, 1 mM DTT, 1 mM phenylmethylsulfonyl fluoride, 0.2 mM CHX, 10 U/ml RNase OUT], centrifuged, resuspended in polysome extraction buffer [400 mM KOAc, 25 mM HEPES, 15 mM $Mg(OAc)_2$, 2% digitonin, 1 mM DTT, 1 mM phenylmethylsulfonyl fluoride, 0.2 mM CHX, 50 U/ml RNase OUT], and incubated on ice for 30 min. After centrifugation for 10 min at 10,000 rpm at 4°C, 800 μl of the supernatant was either layered onto a 10-ml 10 to 50% sucrose gradient and centrifuged at 35,000 rpm for 3 h at 4°C or layered onto a 10-ml 5 to 20% sucrose gradient and centrifuged at 40,000 for 4 h at 4°C. Gradients were fractionated while UV absorbance at 254 nm was monitored. Total RNA was isolated from fractions by use of Trizol-LS reagent and analyzed by agarose gel electrophoresis to detect rRNA. A portion of each sample was used for reverse transcription PCR (RT-PCR) to detect viral RNA as described before (15). Protein was trichloroacetic acid precipitated, solubilized in SDS-PAGE loading buffer, and analyzed by Western blotting following procedures described elsewhere (3).

RESULTS

DRBP76 and NF45 form a binary complex in neuronal cells. DRBP76 is an RNA binding protein capable of associating with and repressing activity of the HRV2 IRES (27). Recent work by multiple labs suggests that DRBP76 acts as a component of a protein complex to regulate gene expression at a posttranscriptional level. DRBP76 is a member of the nuclear factor of activated T cells complex, which consists of DRBP76 and NF45 (25). In addition, it has been characterized in the NFAR complex, comprised of DRBP76, NF45, and RHA (20). All three NFAR members were identified by affinity chromatography to associate with the HRV2 IRES (27). However, this does not necessarily imply association of the intact NFAR complex with the HRV2 IRES in vivo. Therefore, we investigated assembly of these proteins in complexes in the cytoplasm of HEK-293 neuroblasts and glioma cells. The compositions of complexes engaging DRBP76 may differ in a cell-type-specific manner and may influence association with the HRV2 IRES and related effects on IRES-mediated translation.

We used molecular size exclusion chromatography to determine the approximate molecular sizes of complexes containing DRBP76, NF45, and RHA in HEK-293 and HTB-14 cells. In the former, DRBP76 elutes from the column in two distinct peaks; the first peak was detected in the void volume of the column, indicating that a portion of DRBP76 is bound in an unresolvable macromolecular complex. The second peak, at a molecular size of ~140 kDa, overlaps with the single elution peak of NF45 (Fig. 1A), consistent with a DRBP76:NF45 heterodimer (the observed molecular sizes of DRBP76 and NF45 are 90 kDa and 45 kDa, respectively). RHA elutes from the column as a single peak at ~390 kDa, and its distribution does not overlap with DRBP76 or NF45 (Fig. 1A). These data suggest that in HEK-293 cells DRBP76 exists predominantly as a heterodimer with its binding partner NF45. Notably, neither DRBP76 nor NF45 were detected as monomers.

Size exclusion chromatography indicates that DRBP76 assembles in different complexes in HTB-14 cells (Fig. 1A). Apart from a peak in the void volume of the column, DRBP76's elution peak corresponds to a complex with a molecular size of ~370 kDa and does not overlap with the single elution peak for NF45 (at ~170 kDa) (Fig. 1A). The elution profile of RHA was similar to that observed with HEK-293 cell lysates. The elution profiles of RHA, DRBP76, and NF45 are incompatible with the DRBP76:NF45 heterodimer or the

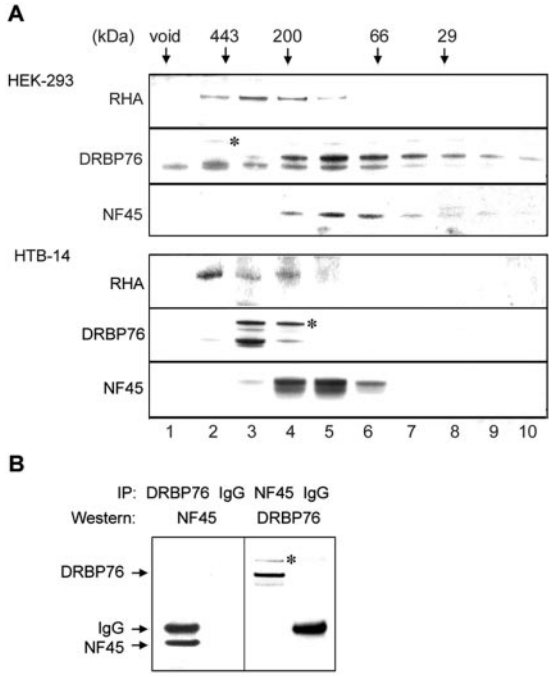

FIG. 1. Molecular size exclusion chromatography. (A) HEK-293 and HTB-14 S10 lysates were applied to a Sepharose matrix under constant pressure. After collection of void volume, 1-ml fractions were collected and protein content was analyzed by SDS-PAGE and Western blotting using α-RHA, α-DRBP76, and α-NF45 antibodies. The column was calibrated with known standards of various molecular sizes, as indicated by arrows. Asterisks denote ILF3, a larger isoform of DRBP76. (B) Coimmunoprecipitation of DRBP76 and NF45 from HEK-293 cells. Immunoprecipitates (IP) were generated with α-DRBP76, α-NF45, and mouse immunoglobulin G (IgG), as indicated. Coprecipitating proteins were analyzed by SDS-PAGE and Western blotting with α-DRBP76 and α-NF45 antibodies.

NFAR complex in HTB-14 cells. We therefore did not further investigate DRBP76-containing complexes in HTB-14 cells by immunoprecipitation.

To confirm formation of the DRBP76:NF45 heterodimer in HEK-293 cells and exclude the possibility of similarly sized complexes involving proteins other then DRBP76 and NF45, we performed coimmunoprecipitation experiments. DRBP76 and NF45 were immunoprecipitated from HEK-293 cell lysates, and the immunoprecipitate was subjected to Western blot analysis to determine retrieval of the heterodimer partner (Fig. 1B). Confirming the size exclusion chromatography results, DRBP76 and NF45 coimmunoprecipitate from a HEK-293 cell lysate (Fig. 1A). Interleukin enhancer-binding factor 3 (ILF3), a larger DRBP76 isoform, which was not identified as an HRV2 IRES binding protein, was also apparent (Fig. 1A and B). Both ILF3 and DRBP76 exist in multiple isoforms, likely due to variable posttranslational modifications (32, 39, 45).

Neuronal DRBP76:NF45 complexes bind to the HRV2 IRES. The IRES binding capacity of DRBP76 is restricted to neuronal cells, as determined by in vitro binding analyses (27). We extended these analyses to study whether the association between the heterodimer and the HRV2 IRES is cell type specific and whether IRES binding of NF45 depends upon DRBP76. Comparative RNA affinity chromatography was performed with HRV2 IRES stem loop domains V/VI by using cytoplasmic extracts from HEK-293 or HTB-14 cells. Bound protein was retrieved by step elution with increasing salt concentrations. In accordance with a previous investigation (27), DRBP76 from HEK-293 cells (Fig. 2A), but not from HTB-14 cells (Fig. 2B), efficiently bound the IRES. Interestingly, the binding characteristics of NF45 mirrored those of DRBP76, as indicated by association of the heterodimer with the HRV2 IRES in neuronal cells (Fig. 2A) but not in glioma cells (Fig. 2B).

Not all of the DRBP76:NF45 heterodimer in HEK-293 cells associated with the HRV2 IRES in our RNA affinity study. Significant amounts of both proteins were found in flowthrough and H200 washes of the affinity column. This observation indicates that (i) the RNA binding capacity of our column is saturated, (ii) a fraction of DRBP76 does not heterodimerize with NF45 and, therefore, is unable to bind to the HRV2 IRES, or (iii) the heterodimer is engaged in competing ribonucleoproteins (RNPs), preventing association with the IRES. Empirical evidence favors the third possibility, because prior micrococcal nuclease treatment of cytoplasmic HEK-293 extracts to remove en-

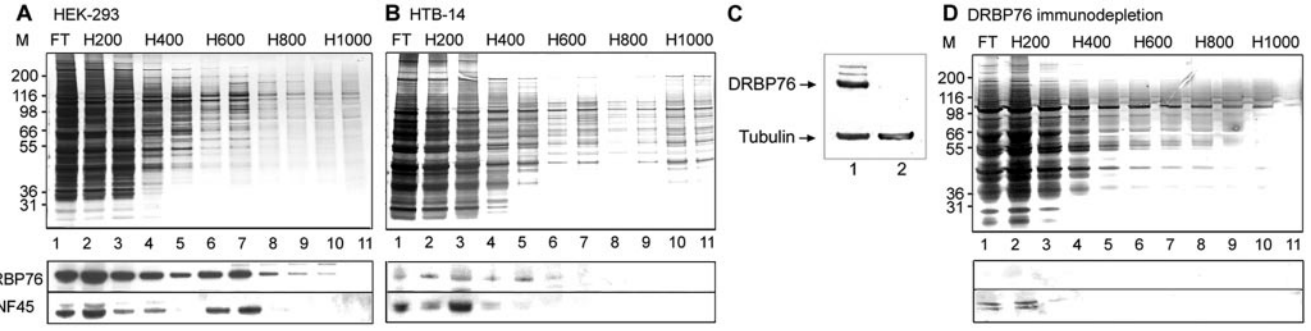

FIG. 2. Comparative RNA affinity chromatography. HEK-293 (A), HTB-14 (B), and DRBP76-immunodepleted HEK-293 (D) S10 lysates were applied to RNA affinity columns. After collection of flowthrough (FT; lane 1), the column was washed with H200 (lanes 2 and 3) and eluted with a 400 to 1,000 mM KCl gradient (lanes 4 to 11). Column fractions were analyzed by SDS-PAGE and silver staining or Western blotting with α-DRBP76 and α-NF45 antibodies, as indicated. (C) Western blot analysis of HEK-293 S10 lysate (lane 1) and DRBP76-immunodepleted HEK-293 S10 lysate (lane 2) by use of α-DRBP76 and α-tubulin antibodies, as indicated. M, molecular size markers in kilodaltons.

dogenous RNA increased the fraction of bound DRBP76:NF45 complex (data not shown).

To discern independent binding of NF45, we investigated IRES affinity in HEK-293 cell extracts devoid of DRBP76. Immunodepletion effectively removed DRBP76, as it was no longer detectable by Western blotting (Fig. 2C). DRBP76 removal disrupted association of NF45 with the HRV2 IRES in neuronal cells (Fig. 2D). DRBP76 immunodepletion is also likely to remove NF45 from extracts; nevertheless, the lack of IRES binding by remnant NF45 in the immunodepleted extract suggests that NF45 is unable to bind independently to the IRES. These data, in addition to observation of the DRBP76:NF45 heterodimer by gel filtration and coimmunoprecipitation, suggest that DRBP76 and NF45 associate with the HRV2 IRES as a complex.

The heterodimer associates with the translation apparatus in neuronal cells. DRBP76 and NF45 are enriched in RSW extracts of neuronal cells compared to those of glioma cells (27). Colocalization of these proteins with ribosomes suggests a role in translation control. To investigate the association of the heterodimer with the translation apparatus, we performed velocity sedimentation analyses of DRBP76 and NF45 in ribosomal profiles in vivo. Cytoplasmic extracts of mock- or virus-infected cells were subjected to density gradient centrifugation followed by fractionation with concomitant analysis of optical density (Fig. 3 and 4). Protein composition was assayed in alternating fractions while rRNA and viral RNA (in infected cells) were analyzed in each fraction. In HEK-293 cells, DRBP76 and NF45 sediment with free protein, 40S and 60S subunits, and mono- and polysomes (Fig. 3A). We excluded the possibility that the proteins cosediment with polysomes due to participation in macromolecular complexes by treating samples with EDTA to disrupt polysomes and release associated RNPs. EDTA disengaged the heterodimer to the top of the gradient, confirming specific association with polysomes (Fig. 3D). RpS6 marks the presence of ribosomes, and tubulin represents free protein.

Translation initiation of PV-RIPO RNA is arrested in neuronal cells. In PV-RIPO-infected HEK-293 cells, viral RNA is detected mainly in 40S-subunit-containing fractions, with lesser signal in mono- and disome peaks (Fig. 3B). Retention of PV-RIPO RNA with 40S ribosomal subunits suggests hindrance of translation initiation at the HRV2 IRES resulting in failure to assemble with polysomes.

Sedimentation of the viral RNA at 40S may indicate either association with 40S ribosomal subunits and a block of subsequent initiation events or participation in translationally inactive nonribosomal RNPs. Indeed, incubation of PV RNA with cytoplasmic extracts alters its inherent sedimentation rate, suggesting the spontaneous formation of RNPs that appeared to be distinct from ribosomal subunits (2, 11). Assembly of PV-RIPO RNA into an RNP including the DRBP76:NF45 heterodimer may thus block translation by preventing recruitment of the 40S ribosomal subunit.

PV-RIPO infection of HEK-293 cells dramatically shifted the sedimentation pattern of DRBP76 and NF45; polysomal association was lost by 4 hpi, at which point DRBP76 and NF45 were detected almost entirely in fractions containing free protein or both 40S subunits and PV-RIPO RNA (Fig. 3B). This effect is not due to a shift of ribosomes from the polysome to the monosome pool, because the relative absorbance pattern did not change significantly upon infection (Fig. 3A and B). This indicates that polysome abundance and the average number of ribosomes per message are not affected by PV-RIPO infection of HEK-293 cells at 4 hpi. Rather, the shift from polysomal to premonosomal fractions may result from virus-induced modification of DRBP76 and NF45 in HEK-293 cells.

The presence of DRBP76:NF45 in the 40S-subunit-containing fractions may be due to specific association with the 40S subunit, formation of 40S RNPs, or spreading from the free-protein-containing fractions, since they overlap in the ribosomal profile (Fig. 3B). To evaluate the latter possibility, we performed fine mapping of the free-protein- and 40S-subunit-containing fractions by low-density gradient velocity sedimentation analysis (Fig. 3C). rRNA and protein were analyzed from every fraction by agarose gel electrophoresis and Western blot analysis, respectively. We were unable to amplify viral cDNA from individual fractions by RT-PCR, most likely due to the diluting effect of increased fractionation. DRBP76 and NF45 were detected both in free-protein-containing fractions (Fig. 3C, lanes 1 to 14) and in 40S-subunit-containing fractions (Fig. 3C, lanes 16 to 24). The spectra and the distributions of RpS6 and 18S rRNA (Fig. 3C) indicate that the 40S subunit is most abundant in lanes 18 to 22, coincident with a peak of DRBP76 and NF45 sedimentation. We conclude from these studies that DRBP76:NF45 complexes in HEK-293 cells associate with 40S ribosomal subunits or 40S RNPs, overlapping the distribution of translationally arrested PV-RIPO genomic RNA (Fig. 3B and C).

In contrast to PV-RIPO, PV's neuropathogenicity is reflected by robust growth in HEK-293 cells (5). In PV-infected HEK-293 cells, viral RNA is associated almost exclusively with polysomes (Fig. 3E). As with PV-RIPO-infected HEK-293 cells, DRBP76 and NF45 shift to premonosomal fractions; however, their distribution in the gradient does not overlap with viral RNA (Fig. 3E).

DRBP76 and NF45 are not associated with ribosomes in glioma cells. DRBP76 and NF45 abundance was significantly lower in ribosome-containing fractions of HTB-14 than in those of HEK-293 cells (Fig. 3A and F), consistent with protein levels in their RSWs (27). NF45 was detected in premonosomal and monosomal fractions, while DRBP76 did not associate with ribosomes at all. Our data suggest that DRBP76 and NF45 associate with the translation apparatus in HEK-293 cells to a greater extent than that in HTB-14 cells. In accordance with efficient viral translation and propagation in glioma cells, the bulk of PV-RIPO RNA associates with polysomes in infected HTB-14 cells (Fig. 3G). Unlike results with HEK-293 cells, virus infection barely affects the distribution of DRBP76 and NF45 in the ribosomal profile of HTB-14 cells. Significantly, there is complete separation of both proteins in premonosomal and monosomal fractions from translating viral RNA in polysomes.

DRBP76 depletion relieves translation arrest at the HRV2 IRES in neuronal cells. To investigate a functional correlation between PV-RIPO translation and sedimentation of the heterodimer, we conducted ribosomal profile analyses of DRBP76-depleted HEK-293 cells (Fig. 4). shRNA was employed to knock down DRBP76 expression by use of a previously established lentivirus delivery strategy (4, 23, 27). DRBP76/ILF3 protein levels

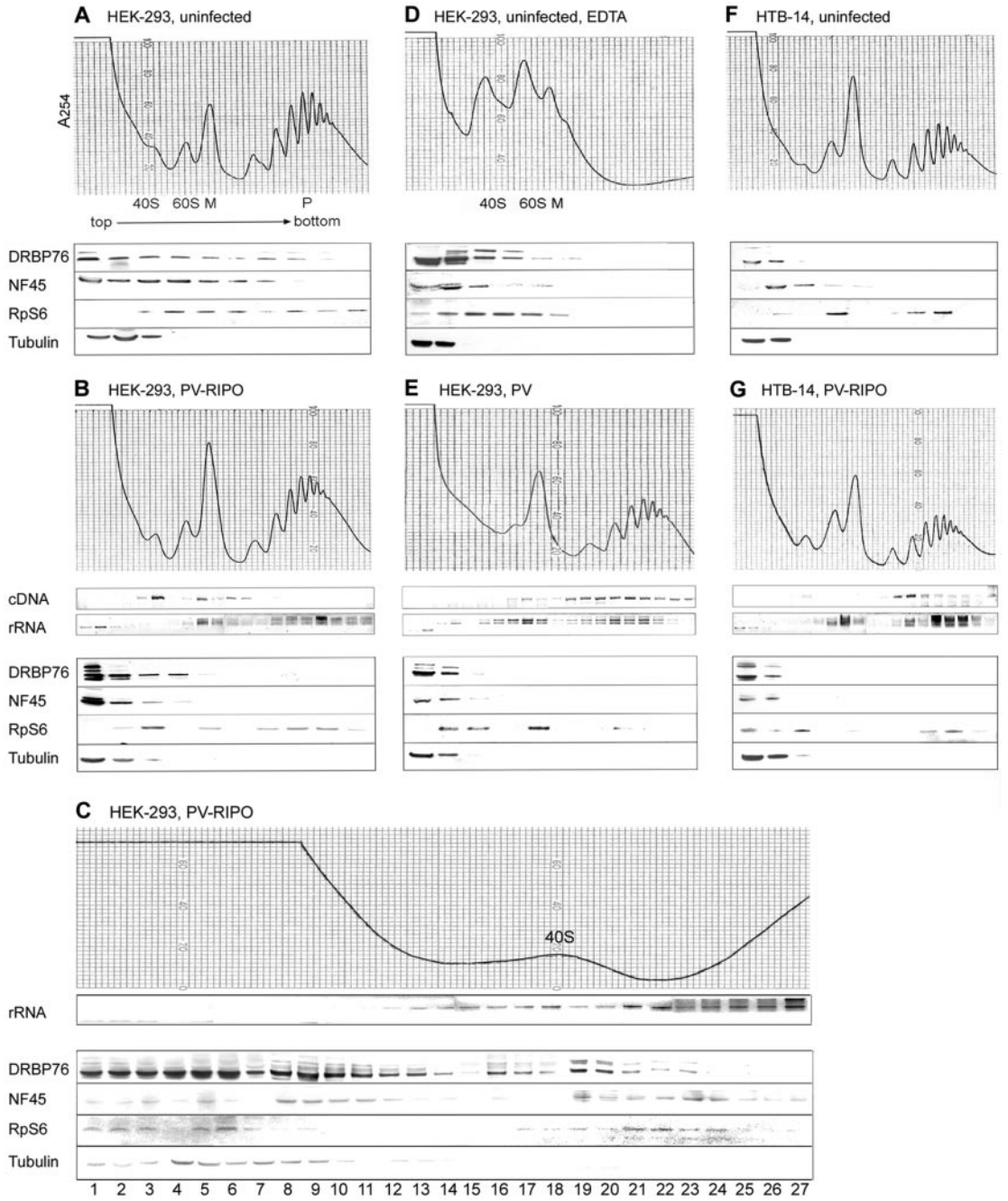

FIG. 3. Ribosomal sedimentation profiles of HEK-293 and HTB-14 cells. (Top panels) A_{254} absorption spectra of 10 to 50% sucrose gradients containing lysates generated from mock-infected HEK-293 cells (A), lysates generated from HTB-14 cells (F), or HEK-293 lysates treated with EDTA (D). (Middle panels) A_{254} absorption spectra of lysates generated from PV-RIPO-infected HEK-293 (B), PV-RIPO-infected HTB-14 (G), or PV-infected HEK-293 (E) cells. (C) A_{254} absorption spectra of a 5 to 20% sucrose gradient containing free protein and 40S ribosomal subunit components from a PV-RIPO-infected HEK-293 cell lysate. Lysates from infected cells were generated at 4 hpi. Western blot analyses were performed with α-DRBP76, α-NF45, α-RpS6, and α-tubulin antibodies, as indicated. Viral cDNA corresponding to the IRES region was amplified by RT-PCR, and rRNA was analyzed from total RNA. M, monosome; P, polysome.

were significantly diminished in HEK-293 cells infected with shRNA-expressing lentivirus (termed shDRBP76 cells [27]) relative to levels in HEK-293 cells infected with lentivirus lacking the shRNA expression cassette (compare Fig. 3A and 4A). Accordingly, in shDRBP76 cells, DRBP76 was removed entirely from ribosomal-subunit-containing fractions (Fig. 4). The knockdown also displaced NF45 from polysomal fractions (Fig. 4B), suggesting that polysome association of NF45 in HEK-293 cells hinges at least in part on DRBP76. As a result, the DRBP76:NF45 sedimentation pattern for shDRBP76 cells resembled that observed for HTB-14 cells (Fig. 3F). DRBP76 depletion in infected HEK-293 cells conversely affected the distribution of PV-RIPO RNA in

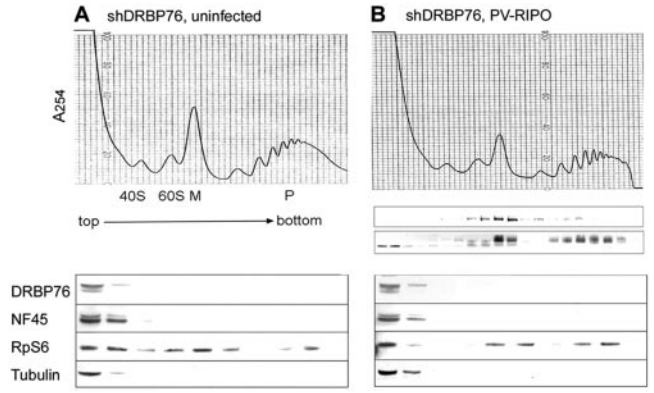

FIG. 4. Ribosomal sedimentation profiles of shDRBP76 cells. A_{254} absorption spectra of 10 to 50% sucrose gradients containing lysates generated from mock-infected (A) or PV-RIPO-infected (B) shDRBP76 cells. Lysates from infected cells were generated 4 hpi and analyzed as described in the legend for Fig. 3. M, monosome; P, polysome.

the ribosomal profile. Displacement of the heterodimer from ribosomal fractions produced a shift of viral RNA towards mono- and polysomal fractions (Fig. 4B). Although the degree of polysome association did not reach that in infected glioma cells, the block of translation initiation in HEK-293 cells was relieved (Fig. 3B and G and 4B). This suggests that DRBP76 depletion and the resulting dissociation of the heterodimer from ribosomes induce assembly of HRV2 IRES-containing viral RNA in polysomes.

DISCUSSION

Insertion of the HRV2 IRES into the PV genome abrogates viral translation and propagation in motor neurons (13) but does not affect growth in glioma (15). Neuroattenuation of the PV-RIPO chimera is due, at least in part, to *trans*-dominant neuronal inhibitors binding to the HRV2 IRES. We previously demonstrated that DRBP76 binds to the HRV2 but not to the PV IRES in neuronal cells (27). Rescue of PV-RIPO growth in neuronal cells by DRBP76 depletion suggests its involvement in *trans*-dominant inhibition of IRES function (27).

We have documented a series of differences between HEK-293 neuroblasts and HTB-14 glioma cells with regard to DRBP76. This protein exists predominantly in a heterodimer with its partner NF45 in the former, but not in the latter. The complex is capable of associating with the HRV2 IRES in neuronal but not in glioma cells. It is enriched in RSW and associates with ribosomes only in neuronal cells. The association of DRBP76 with NF45 may influence its ability to bind to the HRV2 IRES and to associate with the translation apparatus in neuronal cells.

PV-RIPO genomic RNA is retained either with 40S ribosomal subunits or in 40S RNPs in infected neuroblasts but is translation competent in glioma cells, where it assembles into polysomes. The distribution of translationally arrested PV-RIPO RNA overlaps with the DRBP76:NF45 complex in ribosomal profiles. This may implicate the heterodimer:IRES interaction in the repression of HRV2 IRES-driven translation resulting in exclusion from the polysome. Depletion of DRBP76 in neuronal cells also removes NF45 from ribosome-containing fractions, indicating that association with the translation machinery relies on DRBP76 or, alternatively, requires the intact heterodimer. DRBP76 depletion coincides with a shift of PV-RIPO RNA towards polysomal association in infected neuronal cells, corresponding to elevated translation at the HRV2 IRES and significantly enhanced PV-RIPO growth (27). The neuropathogen PV readily propagates in neurons, and DRBP76 depletion has no effect on viral growth or translation via its cognate IRES (27). Accordingly, PV RNA readily assembles into polysomes in infected HEK-293 cells.

Similarly to most translation repressors, the DRBP76:NF45 heterodimer appears to disturb translation initiation events by associating with UTR sequences (10). The locus of DRBP76:NF45 binding within the IRES, stem loop domains V/VI, is in line with a role in translation initiation, since this is the proposed site of ribosome entry (18). Retention of PV-RIPO RNA in premonosomal fractions indicates that translation initiation at the HRV2 IRES is hindered. Most likely, the DRBP76:NF45 heterodimer blocks 40S ribosomal subunit recruitment at the IRES; alternatively, it may affect subsequent initiation events through interaction with the 40S ribosomal subunit.

Our observations link HRV2 IRES function to the availability of the heterodimer and the level of its interaction with the translation apparatus. The mechanisms regulating the RNA binding capacity and ribosome association of DRBP76 and its binding partner(s) have not been characterized. Posttranslational modifications and the extent of engagement in RNPs may control the potential for interaction with viral RNA in a cell-type-specific manner (32, 39, 45). Indeed, gel filtration analyses indicate that cell-type-specific posttranslational modification of DRBP76 may determine its participation in distinct complexes.

Viral RNAs translating under the control of the HRV2 IRES, but not the PV IRES, are excluded from polysomes in neuronal cells but translate efficiently in glioma cells. Our research provides an example of selective recruitment of mRNAs into polysomes due to the cell-type-specific conditions in glioma cells. Specific induction of messages encoding cyclin D1, fibroblast growth factor 2, c-*myc*, and vascular endothelial growth factor in cancer cells has been reported previously (42). Interestingly, these mRNAs are capable of translation via internal ribosomal entry (28, 35, 38, 40), indicating a favorable environment for IRES-mediated translation in cancer cells. More generally, selective polysome assembly on existing mRNAs has recently been described as a main downstream effect of oncogenic Ras/Akt signaling in glioma (36). As exemplified with the HRV2 IRES, the capacity for polysome assembly may be regulated by RNA binding proteins with cell-type-specific distribution, RNA binding properties, and/or association with the translation apparatus.

Our data illustrate how organ-specific and intracellular distribution of translation factors can determine translation, particle propagation, and, hence, pathogenic features of viruses. HRVs do not naturally infect the human central nervous system. However, the major-group HRVs have the capacity to target motor neurons via their cellular receptor intercellular adhesion molecule 1 (7). The absence of neuropathogenicity with these viruses may be due to repression of viral translation by incompatible RNA-protein interactions at the HRV IRES. We are employing the therapeutic utility of glioma-specific translation via the HRV2 IRES with the oncolytic virus prototype PVS-RIPO targeting cancers expressing

the PV receptor CD155 (15). This agent is in preparation for phase I clinical trials with patients with glioblastoma multiforme.

ACKNOWLEDGMENTS

We thank Hubert Amrein, Haifan Lin, and Shelton Bradrick (Duke University) for critical reading of the manuscript and Bryan Cullen, Mariano Garcia-Blanco, Rachel Lerner, and Chris Nicchitta (Duke University) for technical advice. We thank Bryan Cullen for pSUPER, pNL-SIN, pTat, pRev, and pHIT-G plasmids, Jerard Hurwitz (Memorial Sloan Kettering Cancer Center) for α-RHA antibody, and Sven-Erik Behrens (Fox Chase Cancer Center) for α-NF45 antibody.

This work is supported by PHS grants CA87537 and NS20023. M.G. is a recipient of a Burroughs Wellcome Career Award in the Biomedical Sciences. We gratefully acknowledge a Seth Harris Feldman Research Award from The Brain Tumor Society.

REFERENCES

1. **Agol, V. I., E. V. Pilipenko, and O. R. Slobodskaya.** 1996. Modification of translational control elements as a new approach to design of attenuated picornavirus strains. J. Biotechnol. **44:**119–128.
2. **Baltimore, D., and A. S. Huang.** 1970. Interaction of HeLa cell proteins with RNA. J. Mol. Biol. **47:**263–273.

2a. **Bradford, M. M.** 1976. A rapid and sensitive method for the quantitation of microgram quantities of protein utilizing the principle of protein-dye binding. Anal. Biochem. **72:**248–254.

3. **Bradrick, S., R. Walters, and M. Gromeier.** 2006. The HCV 3′ untranslated region or a poly(A) tract promote efficient translation subsequent to the initiation phase. Nucleic Acids Res. **34:**1293–1303.
4. **Brummelkamp, T. R., R. Bernards, and R. Agami.** 2002. A system for stable expression of short interfering RNAs in mammalian cells. Science **296:**550–553.
5. **Campbell, S. A., J. Lin, E. Y. Dobrikova, and M. Gromeier.** 2005. Genetic determinants of cell type-specific poliovirus propagation in HEK 293 cells. J. Virol. **79:**6281–6290.
6. **Dobrikova, E., P. Florez, S. Bradrick, and M. Gromeier.** 2003. Activity of a type 1 picornavirus internal ribosomal entry site is determined by sequences within the 3′ nontranslated region. Proc. Natl. Acad. Sci. USA **100:**15125–15130.
7. **Dufresne, A. T., and M. Gromeier.** 2004. A nonpolio enterovirus with respiratory tropism causes poliomyelitis in intercellular adhesion molecule 1 transgenic mice. Proc. Natl. Acad. Sci. USA **101:**13636–13641.
8. **Evans, D. M., G. Dunn, P. D. Minor, G. C. Schild, A. J. Cann, G. Stanway, J. W. Almond, K. Currey, and J. V. Maizel, Jr.** 1985. Increased neurovirulence associated with a single nucleotide change in a noncoding region of the Sabin type 3 poliovaccine genome. Nature **314:**548–550.
9. **Gebauer, F., M. Grskovic, and M. W. Hentze.** 2003. Drosophila sex-lethal inhibits the stable association of the 40S ribosomal subunit with msl-2 mRNA. Mol. Cell **11:**1397–1404.
10. **Gebauer, F., and M. W. Hentze.** 2004. Molecular mechanisms of translational control. Nat. Rev. Mol. Cell Biol. **5:**827–835.
11. **Girard, M., and D. Baltimore.** 1966. The effect of HeLa cell cytoplasm on the rate of sedimentation of RNA. Proc. Natl. Acad. Sci. USA **56:**999–1002.
12. **Gray, N. K., and M. W. Hentze.** 1994. Iron regulatory protein prevents binding of the 43S translation pre-initiation complex to ferritin and eALAS mRNAs. EMBO J. **13:**3882–3891.
13. **Gromeier, M., L. Alexander, and E. Wimmer.** 1996. Internal ribosomal entry site substitution eliminates neurovirulence in intergeneric poliovirus recombinants. Proc. Natl. Acad. Sci. USA **93:**2370–2375.
14. **Gromeier, M., B. Bossert, M. Arita, A. Nomoto, and E. Wimmer.** 1999. Dual stem loops within the poliovirus internal ribosomal entry site control neurovirulence. J. Virol. **73:**958–964.
15. **Gromeier, M., S. Lachmann, M. R. Rosenfeld, P. H. Gutin, and E. Wimmer.** 2000. Intergeneric poliovirus recombinants for the treatment of malignant glioma. Proc. Natl. Acad. Sci. USA **97:**6803–6808.
16. **Gromeier, M., and A. Nomoto.** 2002. Pathogenesis of picornaviruses, p. 426–443. *In* B. Semler and E. Wimmer (ed.), Picornaviruses. ASM Press, Washington, D.C.
17. **Gromeier, M., D. Solecki, D. D. Patel, and E. Wimmer.** 2000. Expression of the human poliovirus receptor/CD155 gene during development of the central nervous system: implications for the pathogenesis of poliomyelitis. Virology **273:**248–257.
18. **Hellen, C. U., T. V. Pestova, and E. Wimmer.** 1994. Effect of mutations downstream of the internal ribosome entry site on initiation of poliovirus protein synthesis. J. Virol. **68:**6312–6322.
19. **Ida-Hosonuma, M., T. Iwasaki, T. Yoshikawa, N. Nagata, Y. Sato, T. Sata, M. Yoneyama, T. Fujita, C. Taya, H. Yonekawa, and S. Koike.** 2005. The alpha/beta interferon response controls tissue tropism and pathogenicity of poliovirus. J. Virol. **79:**4460–4469.
20. **Isken, O., C. W. Grassmann, R. T. Sarisky, M. Kann, S. Zhang, F. Grosse, P. N. Kao, and S. E. Behrens.** 2003. Members of the NF90/NFAR protein group are involved in the life cycle of a positive-strand RNA virus. EMBO J. **22:**5655–5665.
21. **Jang, S. K., H. G. Krausslich, M. J. Nicklin, G. M. Duke, A. C. Palmenberg, and E. Wimmer.** 1988. A segment of the 5′ nontranslated region of encephalomyocarditis virus RNA directs internal entry of ribosomes during in vitro translation. J. Virol. **62:**2636–2643.
22. **Kawamura, N., M. Kohara, S. Abe, T. Komatsu, K. Tago, M. Arita, and A. Nomoto.** 1989. Determinants in the 5′ noncoding region of poliovirus Sabin 1 RNA that influence the attenuation phenotype. J. Virol. **63:**1302–1309.
23. **Lee, M. T., G. A. Coburn, M. O. McClure, and B. R. Cullen.** 2003. Inhibition of human immunodeficiency virus type 1 replication in primary macrophages by using Tat- or CCR5-specific small interfering RNAs expressed from a lentivirus vector. J. Virol. **77:**11964–11972.
24. **Lerner, R. S., R. M. Seiser, T. Zheng, P. J. Lager, M. C. Reedy, J. D. Keene, and C. V. Nicchitta.** 2003. Partitioning and translation of mRNAs encoding soluble proteins on membrane-bound ribosomes. RNA **9:**1123–1137.
25. **Liao, H. J., R. Kobayashi, and M. B. Mathews.** 1998. Activities of adenovirus virus-associated RNAs: purification and characterization of RNA binding proteins. Proc. Natl. Acad. Sci. USA **95:**8514–8519.
26. **Mendez, R., and J. D. Richter.** 2001. Translational control by CPEB: a means to the end. Nat. Rev. Mol. Cell Biol. **2:**521–529.
27. **Merrill, M. K., E. Y. Dobrikova, and M. Gromeier.** 2006. Cell-type-specific repression of internal ribosome entry site activity by double-stranded RNA-binding protein 76. J. Virol. **80:**3147–3156.
28. **Nanbru, C., I. Lafon, S. Audigier, M. C. Gensac, S. Vagner, G. Huez, and A. C. Prats.** 1997. Alternative translation of the proto-oncogene c-myc by an internal ribosome entry site. J. Biol. Chem. **272:**32061–32066.
29. **Nomoto, A., Y. F. Lee, and E. Wimmer.** 1976. The 5′ end of poliovirus mRNA is not capped with m7G(5′)ppp(5′)Np. Proc. Natl. Acad. Sci. USA **73:**375–380.
30. **Ochiai, H., S. A. Moore, G. E. Archer, T. Okamura, T. A. Chewning, J. R. Marks, J. H. Sampson, and M. Gromeier.** 2004. Treatment of intracerebral neoplasia and neoplastic meningitis with regional delivery of oncolytic recombinant poliovirus. Clin. Cancer Res. **10:**4831–4838.
31. **Ostareck, D. H., A. Ostareck-Lederer, I. N. Shatsky, and M. W. Hentze.** 2001. Lipoxygenase mRNA silencing in erythroid differentiation: the 3′UTR regulatory complex controls 60S ribosomal subunit joining. Cell **104:**281–290.
32. **Parrott, A. M., M. R. Walsh, T. W. Reichman, and M. B. Mathews.** 2005. RNA binding and phosphorylation determine the intracellular distribution of nuclear factors 90 and 110. J. Mol. Biol. **348:**281–293.
33. **Paul, A. V., J. Mugavero, J. Yin, S. Hobson, S. Schultz, J. H. van Boom, and E. Wimmer.** 2000. Studies on the attenuation phenotype of polio vaccines: poliovirus RNA polymerase derived from Sabin type 1 sequence is temperature sensitive in the uridylylation of VPg. Virology **272:**72–84.
34. **Pelletier, J., and N. Sonenberg.** 1988. Internal initiation of translation of eukaryotic mRNA directed by a sequence derived from poliovirus RNA. Nature **334:**320–325.
35. **Prats, A.-C., S. Vagner, H. Prats, and F. Amalric.** 1992. *cis*-acting elements involved in the alternative translation initiation process of human basic fibroblast growth factor mRNA. Mol. Cell. Biol. **12:**4796–4805.
36. **Rajasekhar, V. K., A. Viale, N. D. Socci, M. Wiedmann, X. Hu, and E. C. Holland.** 2003. Oncogenic Ras and Akt signaling contribute to glioblastoma formation by differential recruitment of existing mRNAs to polysomes. Mol. Cell **12:**889–901.
37. **Ren, R. B., E. G. Moss, and V. R. Racaniello.** 1991. Identification of two determinants that attenuate vaccine-related type 2 poliovirus. J. Virol. **65:**1377–1382.
38. **Shi, Y., A. Sharma, H. Wu, A. Lichtenstein, and J. Gera.** 2005. Cyclin D1 and c-myc internal ribosome entry site (IRES)-dependent translation is regulated by AKT activity and enhanced by rapamycin through a p38 MAPK- and ERK-dependent pathway. J. Biol. Chem. **280:**10964–10973.
39. **Smith, W. A., B. T. Schurter, F. Wong-Staal, and M. David.** 2004. Arginine methylation of RNA helicase a determines its subcellular localization. J. Biol. Chem. **279:**22795–22798.
40. **Stein, I., A. Itin, P. Einat, R. Skaliter, Z. Grossman, and E. Keshet.** 1998. Translation of vascular endothelial growth factor mRNA by internal ribosome entry: implications for translation under hypoxia. Mol. Cell. Biol. **18:**3112–3119.
41. **Waggoner, S., and P. Sarnow.** 1998. Viral ribonucleoprotein complex formation and nucleolar-cytoplasmic relocalization of nucleolin in poliovirus-infected cells. J. Virol. **72:**6699–6709.
42. **Watkins, S. J., and C. J. Norbury.** 2002. Translation initiation and its deregulation during tumorigenesis. Br. J. Cancer **86:**1023–1027.
43. **Wimmer, E., C. U. Hellen, and X. Cao.** 1993. Genetics of poliovirus. Annu. Rev. Genet. **27:**353–436.
44. **Wyatt, H. V.** 1993. Provocation paralysis. Lancet **341:**61–62.
45. **Xu, Y. H., and G. A. Grabowski.** 2005. Translation modulation of acid beta-glucosidase in HepG2 cells: participation of the PKC pathway. Mol. Genet. Metab. **84:**252–264.